Scientific Journal of the Ternopil National Technical University
2026, vol. 122, no. 2, pp. 63–69,
ISSN: 2522-4433 Print, ISSN: 2522-4441 Online
https://doi.org/10.35784/ visnyk_tntu2026.02.063

Submitted: 2026-04-06 | Revised: 2026-04-30 | Accepted: 2026-05-26

CC-BY 4.0

Features of the fracture of the control valve rod of a thermal power plant steam turbine

Halyna Krechkovska *****

https://orcid.org/0000-0001-7392-7753

Karpenko Physico-Mechanical Institute of the NAS of Ukraine, Department of Diagnostics of Materials Corrosion-Hydrogen Degradation, Ukraine, krechkovskahalyna@gmail.com

*****Corresponding author krechkovskahalyna@gmail.com

Abstract: *The reasons for the failure of the steam turbine control valve rod after 17 years of operation were analyzed. It was found that its fracture began in several places along the perimeter of the rod, followed by coalescence and subsequent spontaneous failure. Fractographic analysis showed that the crack propagated via a high-temperature fatigue fracture mechanism. Impact toughness, strength, and ductility properties determined on axial steel specimens of the control valve rod complied with regulatory requirements. However, the parameters of transverse specimens made from the rod head were lower. A decrease in all these characteristics was also observed in the high-temperature operating zone compared to the low-temperature zone, indicating more intense metal degradation. The control valve rod had 12091 operating hours and 206 shutdowns, which significantly impacted this process. Macrofractographic analysis showed that the rod fracture occurred because of multiple microcrack initiation in the nitrided layer along the perimeter in the zone of the fillet transition (stress concentrator) between the conical part and the head. Further growth of cracks into the depth of the section and their merging led to sudden fracture. Microfractographic studies confirmed the fatigue mechanism of crack initiation under low-amplitude cyclic loading. At the initial stage, characteristic fatigue grooves were observed, corresponding to the second section of the fatigue kinetic diagram. Their results showed that at a temperature of 540°C, the crack growth rate was* $5 \cdot 10^{-8}$ *m/cycle. The rod fracture occurred due to multi-cycle fatigue, and only at the final stage did signs of low-cycle fracture appear.*

Keywords: *steam turbine rod, steel, failure mechanism, nitrided surface layer, mechanical properties, loading.*

1. INTRODUCTION

The reliability and durability of steam turbine components are largely determined by the performance of critical parts, particularly control valve rods operating under high temperatures, pressures, and cyclic loads [1–3]. As a result of long-term operation, such elements undergo a complex of degradation processes, including creep and thermal fatigue, which affects structural transformations and the accumulation of microdamage, ultimately leading to premature failure [4–8].

Particularly dangerous is the combination of high-temperature exposure with cyclic loading, which promotes the development of fatigue cracks even at low stress amplitudes. Under such conditions, crack initiation often occurs in surface layers or stress-concentration zones, after which the cracks gradually propagate through the material [9, 10]. An additional

risk factor is the presence of hardened surface layers (e.g., nitrided), in which damage can form due to differences in properties and residual stresses with the base metal [11].

Analysis of the causes of fractures in elements of power equipment is important for increasing their service life and improving approaches to diagnosing their technical condition. In particular, fractographic analysis allows to establish the mechanism of fracture, to assess the stages of crack development and the influence of operational factors [12, 13]. In this regard, the study of the mechanism of fracture in the metal of the steam turbine control valve rod is an urgent task aimed at increasing the reliability of power equipment.

2. METHODS

The condition of the control valve rod of the steam turbine of the TPP power unit was analyzed after 12091 h of operation at a pressure of 14 MPa and a temperature of 540°C. The mechanical properties of the rod (near the fracture surface) operated in the high-temperature zone and the upper part of the rod (320 mm from the fracture surface) operated in the low-temperature zone were investigated, and are hereinafter designated as zones I and II, respectively.

The chemical composition of the rod metal was determined on an optical spark spectrometer SPECTROMAX LMF 0.5. Fractographic analysis was carried out on a scanning electron microscope Carl Zeiss EVO-40XVP in the «Center for Electron Microscopy and X-ray Microanalysis» at the Karpenko Physico-Mechanical Institute of NAS of Ukraine.

To determine the impact toughness, Menage-type samples (10 mm ×10 mm × 55 mm) with a V-shaped notch 2 mm deep and 0.1 mm in radius were used. Impact tests on the samples were performed on an IO-5003 pendulum impact tester in accordance with ISO 148-1:2022 [14]. The mechanical properties of the steel under tension were determined in cylindrical samples with a 5 mm diameter and a 25 mm working length. Tensile tests were carried out on an UME-10T testing machine in accordance with ISO 6892-1:2019 [15], ISO 7500-1:2018-02 [16], and ISO 9513 [17]. The deformation rate of the samples was 10–3 s–1. All samples were carefully polished before testing using polishing materials and pastes of varying grain sizes. All mechanical properties were determined by averaging the test results of at least three samples of each category, and their deviations from the average value did not exceed 3–5%.

3. RESULTS

The control valve rod of a steam turbine was investigated, which collapsed at the point of the flare transition from its conical section to the head. The chemical composition of the steel included the following (wt.%): 0.19 C; 0.41Si; 0.74Mn; 9.95Cr; 0.02 S; 0.01P; 0.56 Ni; 0.30 V; 0.92 Mo; 0.37 Nb. The control valve rod is made of heat-resistant alloy steel 18Х11МНФБ (European analog X22CrMoV12-1, according to EN 1.4923) and belongs to the martensitic-ferritic class.

The impact toughness of the steel of the steam turbine control valve rod was analyzed using Charpy specimens with a sharp stress concentrator (radius 0.1 mm), since it more clearly reflects the decrease in resistance to brittle fracture due to operational degradation of the metal under the influence of operational factors (temperature, load, environment, etc.) [18, 19].

The impact toughness values of the metal of the head of the lower part of the rod, which was operated in the high-temperature zone, and its upper part (opposite the fracture), which was operated in the low-temperature zone (Table 1), were analyzed. Transverse and axial samples were studied. The impact toughness KCV (on Charpy samples) of the rod metal in the low-temperature operation zone (its upper part) was 0.93…1.04 MJ/m² and met the requirements of the regulations (KCU ≥ 0.59 MJ/m²). Even in the high-temperature operation

zone (lower part of the rod), the KCV value was 0.63–0.68 MJ/m². Only in transverse samples from the high-temperature operation zone (rod head) was the KCV value (0.35–0.41 MJ/m²) lower than the regulated value. The KCU value is approximately 25% higher than the KCV (since it reflects energy consumption primarily for fracture propagation), so the regulatory requirements were violated only in the transverse samples [20]. In general, the rod metal had sufficient resistance to brittle fracture in the axial direction, but a slightly underestimated value in the transverse direction (KCV ≥ 0.44 MJ/m²). However, it should be noted that the impact toughness values on the transverse samples are lower than on the axial ones, since the energy intensity of delamination along the fibers is lower than across them. This is due to the fact that the fracture of the transverse samples occurred by delamination along the direction of rolling of the rod blanks.

Table 1. Impact toughness of metal from a steam turbine control valve rod.

Specimens' location	Specimens' orientation	KCV, MJ/m^2
I	Transverse	0.35–0.41
	Longitudinal	0.63–0.68
II	Longitudinal	0.93–1.04

A significantly lower impact toughness was noted for the metal operated in the high operating temperature zone (lower part of the rod) compared to the metal operated in the low temperature zone (upper part of the rod). Therefore, this pattern was associated with more intense metal degradation at higher temperatures and the possible strong influence of steam as a hydrogenation medium.

As for the characteristics of both strength and plasticity of the metal from the upper (low-temperature) part of the rod, they are higher than for the metal operated in the high-temperature zone (Table 2). The decrease in all short-term characteristics of the metal from the high-temperature zone of operation was associated with high-temperature degradation of the steel, since the duration of operation of the rod (12091 h), the number of starts (206 starts), the operating temperature (540 °C), the presence of a hydrogenating environment (contact with steam), and cyclic loads with a significant static component are all factors of intensification of structural transformations in steel with the redistribution of carbides to interphase boundaries and grain boundaries. At the same time, it is known that these manifestations of degradation do not improve the high-temperature workability of steels.

Table 2. Mechanical characteristics of 18X11MNFB steel from a damaged control valve rod obtained from tensile testing results.

Specimens' location	Specimens' orientation	σ_{UTS}, MPa	σ_{YS}, MPa	Elongation, %	RA, %
I	Transverse	682	536	7.2	53
	Longitudinal	798	625	17.7	54.2
II	Longitudinal	860	690	18.5	60.5

From the analysis of the data presented in Table 2, it follows that, despite the worse tensile characteristics of the metal from the high-temperature zone of the rod (compared to the characteristics of the metal from its low-temperature zone), they still met the requirements of the GOST 18968-73 regulation ($\sigma_{UTS} \geq 740$ MPa, $\sigma_{YS} \geq 590$–735 MPa, Elongation ≥ 15%, RA ≥ 50%). The characteristics determined on the transverse samples exceeded these limits.

Microfractographic analysis showed that the initiation of a crack in the rod occurred in several places along its perimeter from damage in the surface nitrided layer in the area of the fillet transition between the conical part of the rod and its head (Fig. 1). Damage in the nitrided

layer spread to its entire depth (up to 200 μm) and caused a high concentration of stresses. This created favorable conditions for the propagation of fatigue cracks in the main metal of the rod. Macro-detail of the fracture indicates that fatigue is responsible for the rod failure. Secondary cracks were observed along almost the entire perimeter of the rod at the transition, which is a sign of weak adhesion between them, which was associated with internal oxidation (Fig. 1c).

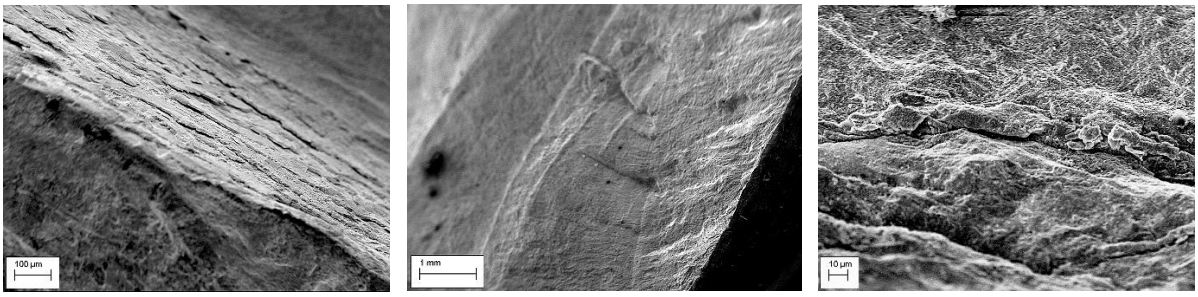

(**a**) (**b**) (**c**)

Figure 1. (**a**, **b**) Crack initiation in different zones around the rod perimeter; (c) secondary cracks on the fracture surface.

The fracture of the rod was analyzed macro-fractographically, and it was found that it collapsed due to multiple microcracks in the nitrided layer along the perimeter of the rod, in the fillet transition zone between its conical part and the head, which acts as a stress concentrator. Further, the crack growth occurred in the depth of the section with the merging of the fronts of separate cracks from the surface and the final spontaneous failure of the rod.

Within the nitrided layer, fatigue failure of the partitions between the fragments separated from the matrix by internal oxidation occurred, with the formation of a grooved relief oriented parallel to the outer surface of the rod and with signs of secondary cracking (Fig. 2 a). In areas corresponding to decohesion zones due to internal oxidation, traces of corrosion effects on the interphase boundaries between the matrix and inclusions of various nature were identified.

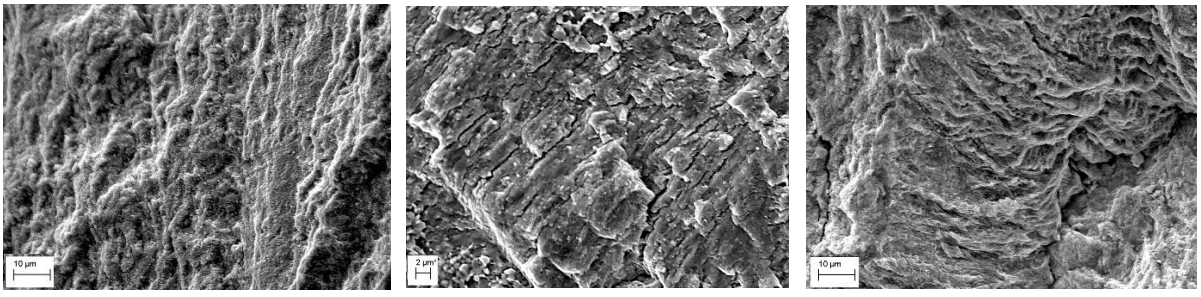

(**a**) (**b**) (**c**)

Figure 2. Microfractograms of rod fracture: (a) in the area of the surface nitrided layer; (b) at the stage of stable fracture propagation; (c) in the crack growth zone with high asymmetry of the loading cycle (at the stage of low-cycle fatigue).

At the initial stage of the transition of the fracture to the base metal, fatigue cracks originated from the blunted crack tip in the nitrided layer by forming a smooth relief with barely noticeable fatigue grooves. By the step of the grooves, it was established that at the initial stage of crack growth in the rod, their speed was 5·10-8 m/cycle. With increasing crack length, the contours of the grooves became increasingly clear, their step became larger, and the festoons, the surface of which was covered by the grooves, became more

relief. These are signs of an increase in the crack growth rate. The classical groove mechanism of fatigue failure was preserved in most of the rod fractures, which is usually considered a sign of multi-cycle fatigue (Fig. 2 b). Of course, the deeper the fracture spread from the lateral surface of the rod, the greater the pitch of the grooves, the deeper and clearer the secondary cracks that decorated them, and the greater the relief of the festoons.

Along the perimeter of the rod fracture, there were also areas where the fracture from the nitrided layer spread into the base metal much later and had characteristic signs of low-cycle fatigue. At the same time, no secondary cracking was observed at the interface between the nitrided layer and the base metal, but only a blunting of the crack tip in the nitrided layer.

Fatigue fracture in the base metal occurred with significant signs of plastic deformation, delamination, formation of chevron patterns, and track marks (Fig. 2c). It was assumed that the prerequisites for such a fracture arose due to the deepening of cracks in other places along the perimeter of the rod under conditions of multi-cycle fatigue. As a result of low-cycle fatigue, only the alignment of the fracture front occurred.

Thus, based on the study of the microfractographic features of the control valve rod fracture, it was concluded that it occurred as a result of the nucleation of circular microcracks in the nitrided layer due to its internal oxidation and the destruction of the partitions between the oxidized areas due to cyclic loading of the rod caused by vapor pressure drops, flow turbulence and resonance phenomena, when the natural frequency of oscillations of the rods coincides with the frequency of oscillations caused by the influence of technological factors. The high concentration of stresses at their tops, low resistance to high-temperature oxidation, and matrix destruction (due to the release of chromium carbides and a decrease in its content in the matrix) contributed to their germination into the rod base by the mechanism of multi-cycle fatigue. If the niobium present in the steel composition had performed its assigned function (to prevent a decrease in the chromium content in the matrix), the rod resource would have been much greater. Therefore, in the future, to prevent unforeseen damage to such critical structural elements as rods, incoming inspection of the steel structure is recommended.

4. CONCLUSIONS

The mechanical strength, ductility, and impact toughness of the rod steel met the regulatory requirements. Only the properties of transverse specimens made from the head were below the specified values. Furthermore, it was noted that the mechanical properties of the rod steel in the high-temperature operating zone were lower than in the low-temperature operating zone, attributed to more severe metal degradation at high temperatures.

The rod was destroyed due to multiple microcracks originating in the nitrided layer along its perimeter in the area of the fillet transition between its conical part and the head as a stress concentrator, their subsequent growth into the depth of the section with the merging of the fronts of individual surface cracks, and the final spontaneous destruction of the rod.

Microfractographic studies of the fracture showed that the initiation of cracks in the rod occurred by the fatigue mechanism due to low-amplitude cyclic loads. At the stage of crack initiation at the rod fracture, classical fatigue grooves were observed, which are characteristic elements of fatigue failure in the so-called second section of the kinetic diagram of fatigue failure. By the step of the grooves, it was established that at the initial stage of crack growth in the rod at a temperature of 540°C, their speed was $5 \cdot 10^{-8}$ m/cycle. The classical groove mechanism of fatigue failure was observed throughout most of the rod fracture, consistent with multi-cycle fatigue, and only at the final stage of failure were typical signs of low-cycle fatigue observed.

Author Contributions: Conceptualization, Methodology, Writing – original draft, Review & editing, Supervision were performed by Halyna Krechkovska.

Acknowledgments: Generally, the last paragraph of the paper is the place to acknowledge people, organizations, or institutions that provided significant support during the research but do not meet the criteria for authorship.

Funding: This research was funded by a grant from the President of Ukraine, provided by the National Research Foundation of Ukraine, Grant № 2025.02/0031.

Conflicts of Interest: Author Halyna Krechkovska is an associate editor for the Scientific Journal of the Ternopil National Technical University and was not involved in the editorial review or the decision to publish this article.

Data Availability Statement: Data available on request: «The data that support the findings of this study are available from the corresponding author upon reasonable request».

REFERENCES

[1] Yuan Zhanhong and Zhongjin Gao (2024) Analysis and improvement practice for stream control valve rod fracture of back pressure steam turbine. International Core Journal of Engineering, 10, Is. 11, pp. 58–66. https://doi.org/10.6919/ICJE.202411_10(11).0008.

[2] Tkachuk Yu. M., Student O. Z. (2009) Problems of thermal power engineering of Ukraine: analysis of the causes of damage to steam turbine components. Scientific notes, 26, pp. 329–333. http://nbuv.gov.ua/UJRN/Nn_2009_26_68/. (In Ukrainian).

[3] Koliadiuk A. S., Shulzhenko M. H., Hubskyi O. M. (2021) Strength and service life of a steam turbine stop and control valve body. J. of Mechanical Engineering – Problemy Mashynobuduvannia, 24, Is. 4, pp. 61–70. https://doi.org/10.15407/pmach2021.04.061.

[4] Ipohorski M., Luppo M. I., Castillo-Guerra R., Ovejero-García J. (2003) Failure analysis of a steam valve rod. Materials Characterization, 50, is. 1, pp. 23–30. https://doi.org/10.1016/S1044-5803(03)00105-0.

[5] Weng S., Huang Y., Lin S., Xuan F.-Z. (2022)Stress-corrosion crack propagation in nuclear steam turbine rotor steels: effects of microstructure in a simulated environment. Journal of Materials Research and Technology, 17, pp. 725–742. https://doi.org/10.1016/j.jmrt.2022.01.020.

[6] Du C., Liu C., Li X., Lu J., Yuan J. and Liu B. (2023) Fatigue fracture failure analysis of guide valve based on welding defects. Front. Mater, 10, 1298138. https://doi.org/10.3389/fmats.2023.1298138.

[7] Solovey P., Krechkovska H., Student O. (2025) Structural-fractographic indicators of operational damage in steam turbine rotor disc steel. Scientific Journal of TNTU, 4 (120), pp. 90–98. https://doi.org/10.33108/visnyk_tntu2025.04. 090.

[8] Guo F., Lyu Y., Duan Z., Fan Z., Li W., Chen F. (2023) Analysis of regulating valve rod fracture in a petrochemical plant. Processes, 11, 1106. https://doi.org/10.3390/pr11041106.

[9] Solovei P., Student O., Svirska L., Kurnat I., Krechkovska S., Gural T., (2023) Establishing the causes of premature damage of steam turbine rotor blades of TPP. Scientific Journal of the Ternopil National Technical University, 2, 110. https://doi.org/10.33108/visnyk_tntu2023.02 ISSN 2522-4433.

[10] Guiyan Gao, Shusheng Guo and Derui Li. A, (2024) Review of Cavitation Erosion on Pumps and Valves in Nuclear Power Plants, Materials, 17, Is. 5, art. no. 1007. https://doi.org/10.3390/ma17051007.

[11] Terent V. F., Kolmakov A. G., Kvedaras V., Čiuplys V., Antanas Čiuplys, Vilys J., Baikov A. A. (2007) The effect of nitriding on fatigue strength of structural alloys. Mechanika, 64, is. 2, pp. 12–22. https://doi.org/10.5755/j02.mech.14797.

[12] Krechkovs'ka H. V. (2016) Fractographic signs of the mechanisms of transportation of hydrogen in structural steels. Materials Science, 51, is.4, pp. 509–513. https://doi.org/10.1007/s11003-016-9869-5.

[13] Nemchuk O. O., Krechkovska H. V. (2019) Fractographic substantiation of the loss of resistance to brittle fracture of steel after operation in the marine gantry crane elements. Metallofizika I Noveishie Tekhnologii, 41, 6, pp. 825–836. https://doi.org/10.15407/mfint.41.06.0825.

[14] ISO 148-1:2016, Metallic Materials–Charpy Pendulum Impact Test–Part 1: Test Method. ISO: Geneva, Switzerland, 2016, 29 p.

[15] ISO 6892-1:2019, Metallic Materials Tensile Testing. Part 1. Method of Test at Room Temperature. ISO: Geneva, Switzerland, 2020, 70 p.

[16] ISO 7500-1:2018-02, Metallic Materials–Calibration and Verification of Static Uniaxial Testing Machines-Part 1: Tension/Compression Testing Machines–Calibration and Verification of the Force-Measuring Syrod. ISO: Geneva, Switzerland, 2018, 18 p.

[17] ISO 9513, Metallic Materials–Calibration of Extensometer Syrods Used in Uniaxial Testing. ISO: Geneva, Switzerland, 2012, 45 p.

[18] Kori T. H., Kassaye F. T., Kozłowska A., Grajcar A. (2025) Numerical Modeling of Charpy Impact Toughness Behavior and Stress Distribution of Quenching and Partitioning Steel, Symmetry 17, 53. https://doi.org/10.3390/sym17010053.

[19] Michael May (2016) Measuring the rate-dependent mode I fracture toughness of composites – A review, Composites Part A: Applied Science and Manufacturing, 81, pp. 1–12. https://doi.org/10.1016/j.compositesa.2015.10.033.

[20] Krechkovs'ka H. V., Student O. Z., (2017) Determination of the Degree of Degradation of Steels of Steam Pipelines According to Their Impact Toughness on Specimens with Different Geometries of Notches. Materials Science, 52, is. 4, pp. 566–571. https://doi.org/10.1007/s11003-017-9991-z.